Arabian Journal of Chemistry (2017) **10**, 389–397

King Saud University

Arabian Journal of Chemistry

www.ksu.edu.sa
www.sciencedirect.com

ORIGINAL ARTICLE

Synthesis, characterization and molecular modeling of new ruthenium(II) complexes with nitrogen and nitrogen/oxygen donor ligands

Ahmed A. Soliman [a,*], Mina A. Amin [a], Ahmed A. El-Sherif [a,b], Cigdem Sahin [c], Canan Varlikli [d]

[a] *Department of Chemistry, Faculty of Science, Cairo University, 12613 Giza, Egypt*
[b] *Department of Chemistry, Faculty of Arts and Science, Northern Border University, Saudi Arabia*
[c] *Department of Chemistry, Art & Science Faculty, Pamukkale University, Denizli, Turkey*
[d] *Ege University, Solar Energy Institute, 35100 Bornova, Izmir, Turkey*

Received 10 November 2014; accepted 2 April 2015
Available online 8 April 2015

KEYWORDS

Ruthenium(II);
Spectroscopy;
Thermal stability;
Molecular modeling

Abstract Ru(II) complexes with some dinitrogen ligands; 3,4-diamino benzoic acid (DABA), 2-hydazinopyridine (hzpy), 2,2′-bipyridyl (bipy) and anthranilic acid (anth) have been synthesized and characterized by using IR, mass, and UV–Vis spectrometry and thermal analysis. The thermodynamic parameters (ΔE, ΔH, ΔS and ΔG) have been calculated by using Coats–Redfern and Horowitz–Metzger methods. The electrochemical properties of these complexes have been studied by using cyclic voltammetry. The evaluated energies of the HOMO and LUMO are in the range of −4.94 to −4.85 eV and −2.86 to −2.68 eV, respectively. The complexes have been proven to have an octahedral geometry with DABA, hzpy and bipy as N2 donor ligands and NSC as monodentate ligand. The structure of the Ru(II) complexes has been geometrically optimized by using parameterized PM3 semiempirical method.

1. Introduction

Metal complexes containing nitrogen chelating ligands have interesting physicochemical properties and important biological activities (Ali and Livingstone, 1974; Campbell, 1975; Crichton, 2012; Padhye and Kauffman, 1985). The transition metal ruthenium has a rich chemistry (McCleverty and Meyer, 2004; O'Regan and Grätzel, 1991). This allows the utilization of its complexes, such as ruthenium(II) polypyridyl complexes, in dye sensitized solar cells (DSSCs) (Kalyanasundaram and Grätzel, 1998; Gratzel, 2004;

Abbreviations: Hzpy, 2-hydrazinopyridine hydrochloride; DABA, 3,4-diaminobenzoic acid; Bipy, 2,2′-bipyridine; DSSC, dye sensitized solar cell; MLCT, metal-ligand charge transfer

* Corresponding author. Tel.: +20 1004817251; fax: +20 235727556.
E-mail address: ahmedsoliman61@gmail.com (A.A. Soliman).
Peer review under responsibility of King Saud University.

Production and hosting by Elsevier

http://dx.doi.org/10.1016/j.arabjc.2015.04.001

Nazeeruddin et al., 1993; O'Regan and Grätzel, 1991; Sahin et al., 2010a,b), molecular electronic devices (Robertson and McGowan, 2003), organic light emitting diodes (Oner et al., 2012), DNA structural probes and new antitumor agents (Dos Santos et al., 2013; Metcalfe and Thomas, 2003). Recently, depending on massive data on ruthenium polypyridyl complexes, the replacement of 2,2′-bipyridine (bipy) by other ligands with nitrogen-containing heterocyclic compounds, has received attention as this causes changes in their photophysical and electrochemical properties (Balzani et al., 1996; Chao and LN, 2005; De Cola and Belser, 1998; Juris et al., 1988; Kaes et al., 2000; Vos and Kelly, 2006). These properties actually represent the most important factors on their performances in relative application areas. In this study, we prepared five new ruthenium complexes by using anthranilic acid (anth), 3,4-diaminobenzoic acid (DABA), 2-hydrazinopyridine (hzpy) and 2,2′-bipyridyl (bipy) as the ligands and investigated their structural, thermodynamic, optical and electrochemical properties.

2. Experimental

2.1. Materials

All chemicals used in this study were of the highest purity available. 3,4-diaminobenzoic acid was purchased from Arcos Organics, ruthenium trichloride hydrate was purchased from Merck while, 2,2′-bipyridine, 2-hydrazino pyridine, anthranilic acid, dichloro(p-cymene)ruthenium(II) dimer, ethanol, *N*,*N*-dimethylformamide (DMF), tetrabutyl ammonium hexafluorophosphate ($TBAPF_6$) and methanol were purchased from Sigma–Aldrich. The structural formulas of the investigated ligands are given in Scheme 1.

2.2. Measurements

Infrared measurements of the complexes were taken by using Jasco FT-IR – 460 plus (range 400–4000 cm^{-1}). Mass spectra were taken with a Jeol JMS-AX500 mass spectrometer. Thermal analysis of the complexes was carried out by using a Shimadzu thermo-gravimetric analyzer TGA-50H; under a nitrogen atmosphere with a heating rate of 10 °C/min over a temperature range from room temperature up to 1000 °C. UV–Vis and fluorescence spectra were recorded in a 1 cm path length quartz cell by using an Analytic Jena S 600 UV diode array spectrophotometer and Edinburgh FLS920P fluorescence spectrometers, respectively. Electrochemical data were obtained using a CH Instrument 660 B Model Electrochemical Workstation. Cyclic voltammograms were measured in a cell containing a glassy carbon working electrode, silver wire reference electrode, platinum wire counter electrode and supporting electrolyte consisting of 0.1 M $TBAPF_6$ in DMF (scan rate 100 mV s^{-1}).

2.3. Synthesis of complexes

2.3.1. [Ru(II)(bipy)(DABA)(NCS)$_2$] (*I*)

0.1 g (0.16 mmol) of $[RuCl_2(p\text{-cymene})]_2$ was dissolved in 100 ml of methanol and a few drops of DMF mixture, and then 0.049 g (0.32 mmol) of bipy and 0.097 g (0.64 mmol) of DABA were added to this solution and heated under argon atmosphere at 65 °C for 4 h with constant stirring. This reaction resulted in the formation of a violet precipitate. The precipitated complex was filtered and dried under vacuum and kept in a vacuum desiccator (0.12 g; yield: 71.4%). ^{1}H NMR (DMSO-d_6) δ ppm: 9.39 (d, J = 5.2 Hz, 2H), 8.75 (d, J = 8.4 Hz, 2H), 8.35 (d, J = 4.4 Hz, 1H), 8.29 (t, J = 8.0 Hz, 2H), 7.79 (t, J = 6.4 Hz, 2H), 6.30 (d, J = 6.0 Hz, 2H), 6.05 (d, J = 6.8 Hz, 2H).

2.3.2. [Ru(II)(DABA)(hzpy)(NCS)$_2$] (*II*)

0.2 g (0.32 mmol) of $[RuCl_2(p\text{-cymene})]_2$ was dissolved in 100 ml of methanol and a few drops of DMF mixture, and then 0.0972 g (0.64 mmol) of DABA and 0.116 g (0.64 mmol) of hzpy were added to this solution and heated under argon atmosphere at 65 °C for 4 h with constant stirring. This reaction resulted in the formation of a black precipitate. The precipitated complex was dried under vacuum and kept in a vacuum desiccator (0.110 g; yield: 35.9%). ^{1}H NMR (DMSO-d_6) δ ppm: 8.30 (s, 1H), 7.93 (s, 1H) 7.26 (s, broad, 2H), 6.95–7.17 (m, 5H), 2.65 (s, 1H), 2.31 (s, 1H).

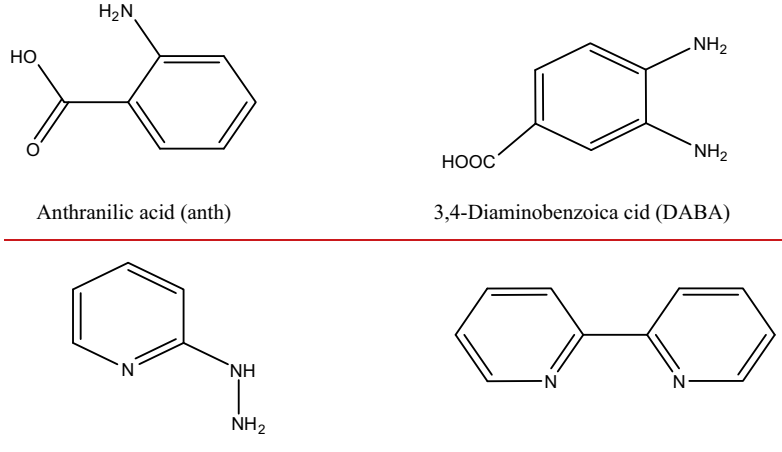

Anthranilic acid (anth) 3,4-Diaminobenzoica cid (DABA)

2-Hydrazinopyridine (hzpy) 2,2'-bipyridyl (bipy)

Scheme 1 Structural formulas of the investigated ligands.

Table 1 IR spectra of the ruthenium(II) complexes.

Complex	V(N—H) cm^{-1}	V(SCN—)cm^{-1}	V(C═N) cm^{-1}	($\rho_t NH_2$)	($\rho_w NH_2$)	($\rho_r NH_2$)	ν(M—N)	ν(M—O)
2-Hydrazinopyridine (hzpy)	3305 and 3256	–	1602	1284	1154	771	–	–
2,2′-Bipyridine (bipy)	–	–	1660	–	–	–	–	–
3,4-Diaminobenzoic acid (DABA)	3328 and 3209	–	–	1211	1153	783	–	–
Anthranilic acid (anth)	3323 and 3238	–	–	1232	1139	761	–	–
[Ru(II)(bipy)(DABA)$(NCS)_2$] **I**	3433	2125	1606	1209	1078	763	555	–
[Ru(II)(DABA)(hzpy)$(NCS)_2$] **II**	3422	2092	–	1236	1031	766	603	–
[Ru(II)$(DABA)_2$(hzpy)]Cl_2 **III**	3415	–	–	1226	–	764	599	–
[Ru(II)(bipy)$(anth)_2$] **IV**	3422	–	1599	1232	1154	766	–	652
[Ru(II)(bipy)$(DABA)_2$]Cl_2 **V**	3420	–	1608	1203	–	767	619	–

Table 2 Mass spectra of the isolated ruthenium(II) complexes.

Complex	M. wt.	Important mass fragmentations (*m*/z)
[Ru(II)(bipy)(DABA)$(NCS)_2$] **I**	525.57	522 (M—3H), 373 (Ru(DABA)$(NCS)_2$ = 374, 217 (Ru$(NCS)_2$ = 217, 151 (DABA-1), 156 (bipy), 58 (NCS), stable Ru isotopes (96, 98, 99, 101, 102, 104)
[Ru(II)(hzpy)(DABA)$(NCS)_2$] **II**	478.51	478 (M^+), 324 (Ru(hzpy)$(NCS)_2$ = 326), 109 (hzpy), 369 (Ru(DABA)$(NCS)_2$ = 369), 152 (DABA), 58 (NCS), stable Ru isotopes (96, 98, 99, 101, 102, 104)
[Ru(II)(hzpy)$(DABA)_2$]Cl_2 **III**	585.41	584 (M—H), 405 (Ru$(DABA)_2$ = 405), 170 (RuCl_2 = 171) 324 (Ru(DABA)Cl_2 = 324), 362 (Ru(DABA)(hzpy) = 362), stable Ru isotopes (96, 98, 99, 101, 102, 104)
[Ru(II)$(Anth)_2$(bipy)] **IV**	529.51	526 (M—3H), 136 (Anth = 137), 156 (bipy), stable Ru isotopes (96, 98, 99, 101, 102, 104)
[Ru(II)$(DABA)_2$(bipy)]Cl_2 **V**	632.46	632 (M^+), 152 (DABA), 156 (bipy), stable Ru isotopes (96, 98, 99, 101, 102, 104)

Table 3 Thermogravimetric analytical data for decomposition of Ru(II) complexes.

Molecular formula	M.W	DTG_{max} K	Decomposition temperature K	Weight loss %	Mass loss		Eliminated species	Metallic residue
					Cal	Found		
[Ru(II)(bipy)(DABA)$(NCS)_2$] **I**	525.57	403.23	347.40–609.48	41.31	214.22	217.11	bipy($C_{10}H_8N_2$) and NCS	Ru
($C_{19}H_{16}N_6O_2S_2Ru$)		633.97	609.48–689.35	40.35	210.22	212.06	DABA($C_7H_8N_2O_2$) and NCS	18.34% (19.21%calc.)
[Ru(II)(hzpy)(DABA)$(NCS)_2$] **II**	478.51	289.02	327.80–568.52	44.66	210.2	213.7	DABA($C_7H_8N_2O_2$) and NCS	Ru
($C_{14}H_{15}N_7O_2S_2Ru$)		613.44	568.52–695.22	34.87	167.19	166.85	hzpy($C_5H_7N_3$) and NCS	20.47% 21.12%calc.
[Ru(II)(hzpy)$(DABA)_2$]Cl_2 **III**	585.41	304.97	294.23–515.02	15.37	95.1	89.97	$3NH_3$ and CO_2	RuO_2
($C_{19}H_{23}N_7O_4S_2Cl_2Ru$)		540.19	515.02–665.20	62.24	357.24	364.39	($C_{18}H_{14}N_4Cl_2$)	22.39% 22.73%calc.
[Ru(II)$(Anth)_2$(bipy)] **IV**	529.51	380.29	314.25–594.59	18.43	95.1	97.58	$3NH_3$ and CO_2	RuO_2
($C_{24}H_{20}N_4O_4Ru$)		605.07	594.59–733.22	57.18	301.34	302.77	($C_{23}H_{11}NO_2$)	24.39% 25.14%calc.
[Ru(II)$(DABA)_2$(bipy)]Cl_2 **V**	632.46	344.64	328.07–600.81	28.34	188.47	179.23	DABA and HCl	Ru
($C_{24}H_{24}N_6O_4Cl_2Ru$)		618.74	600.81–651.94	56.71	342.78	358.66	$C_{17}H_{15}ClN_4O_2$	14.94% 15.98%calc.

*2.3.3. [Ru(II)(DABA)$_2$(hzpy)]Cl$_2$ (**III**)*

0.31 g (0.50 mmol) of [$RuCl_2$(p-cymene)]$_2$ was dissolved in 100 ml of methanol and a few drops of DMF mixture, and then 0.304 g (2.0 mmol) of DABA and 0.182 g (1.0 mmol) of hzpy were added to this solution and heated under argon atmosphere at 65 °C for 4 h with constant stirring. This reaction resulted in the formation of a black precipitate. The precipitated complex was dried under vacuum and kept in a

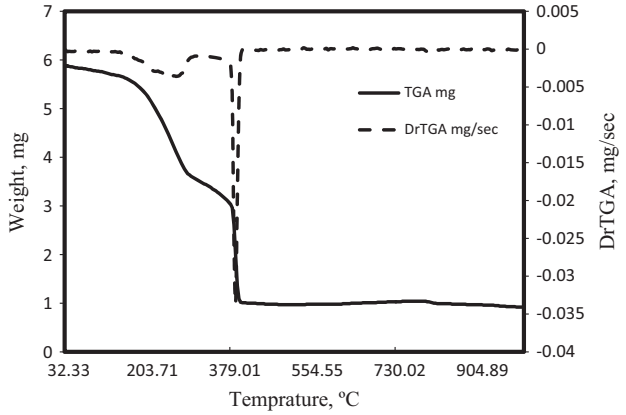

Figure 1 TGA and DrTGA curves of complex **I**.

vacuum desiccator (0.236 g; yield: 40.3%). ^{1}H NMR (DMSO-d_6) δ ppm: 8.30 (s, 2H), 7.24 (m, 4H), 7.11 (m, 4H), 6.98 (m, 4H), 2.87 (s, 1H), 2.71 (s, 1H).

2.3.4. *[Ru(II)(bipy)(anth)$_2$] (**IV**)*

0.31 g (0.50 mmol) of [RuCl$_2$(p-cymene)]$_2$ was dissolved in 100 ml of methanol and a few drops of DMF mixture, and then 0.156 g (1.0 mmol) of bipy and 0.274 g (2.0 mmol) of anthracene were added to this solution and heated under argon atmosphere at 65 °C for 4 h with constant stirring. This reaction resulted in the formation of a black precipitate. The precipitated complex was dried under vacuum and kept in a vacuum desiccator (0.200 g; yield: 37.8%).

2.3.5. *[Ru(II)(bipy)(DABA)$_2$]Cl$_2$ (**V**)*

0.31 g (0.50 mmol) of [RuCl$_2$(p-cymene)]$_2$ was dissolved in 100 ml of methanol and a few drops of DMF mixture, and then 0.304 g (2.0 mmol) of DABA and 0.156 g (1.0 mmol) of bipy were added to this solution and heated under argon atmosphere at 65 °C for 4 h with constant stirring. This reaction resulted in the formation of a deep brown precipitate. The precipitated complex was dried under vacuum and kept in a vacuum desiccator (0.132 g; yield: 20.8%).

2.4. Molecular modeling

An attempt to gain a better insight into the molecular structure of the synthesized ruthenium complexes, geometric optimization and conformation analysis has performed by using a semiempirical parameterized PM3 method as implemented in HyperChem 7.5 (HyperChem version 7.5 Hypercube, Inc., 2003). A gradient of 1×10^{-2} cal Å^{-1} mol^{-1} was set as a convergence criterion in all the quantum calculations.

3. Results and discussion

3.1. IR spectra

The IR spectra of the complexes are compared with the free ligands (hzpy, bipy, Anth and DABA) in order to determine and monitor the change in the vibration frequency of the coordination sites that are involved in chelation. The characteristic peaks of all ligands and its complexes are listed in Table 1. The FT-IR spectra of the diamine ligands showed medium to strong bands at (3390–3305) cm^{-1} and (3324–3209) cm^{-1} which are assigned to stretching vibration of the NH$_2$ (hzpy, Anth and DABA) groups. These anti-symmetric and symmetric stretching bands appeared as a broad band in each spectrum with higher frequencies ranging between 3433 and 3415 cm^{-1} indicating the coordination of these groups to metal ions. The coordination of the NH$_2$ or NH groups is also confirmed from the shift of their

Table 4 The thermodynamic data of the thermal decompositions of Ru(II) complexes.[a]

Complex	Decomposition temperature (K)	ΔE (kJ mol^{-1})	R^2	ΔS (J K^{-1} mol^{-1})	ΔH (kJ mol^{-1})	ΔG (kJ mol^{-1})
[Ru(II)(bipy)(DABA)(NCS)$_2$]	347.40–609.48	25.96	0.98	−210.39	22.6	107.44
	609.48–689.35	27.69	0.85	−265.08	22.41	190.47
		53.65		−475.47	45.01	297.91
[Ru(II)(hzpy)(DABA)(NCS)$_2$]	327.80–568.52	16.57	0.91	−223.62	14.17	78.8
	568.52–695.22	9.51	0.9	−270.47	4.41	170.33
		26.08		−494.09	18.58	249.13
[Ru(II)(hzpy)(DABA)$_2$]Cl$_2$	294.23–515.02	14.98	0.84	223.99	12.44	80.75
	515.02–665.20	2.87	0.74	291.78	0.268	312
		17.85		515.77	12.7	236.75
[Ru(II)(Anth)$_2$(bipy)]	314.25–594.59	14.84	0.92	−238.28	11.66	102.29
	594.59–733.22	29.32	0.72	−228.82	24.29	162.74
		44.16		−467.1	35.95	265.03
[Ru(II)(DABA)$_2$(bipy)]Cl$_2$	328.07–600.81	10.49	0.83	−247.08	7.62	92.78
	600.81–651.94	4.01	0.73	−286.14	−1.12	175.92
		14.5		−533.22	6.46	268.7

[a] Average values of ΔE, ΔS, ΔH and ΔG for the decomposition steps calculated by the Coats–Redfern and Horowitz–Metzger methods.

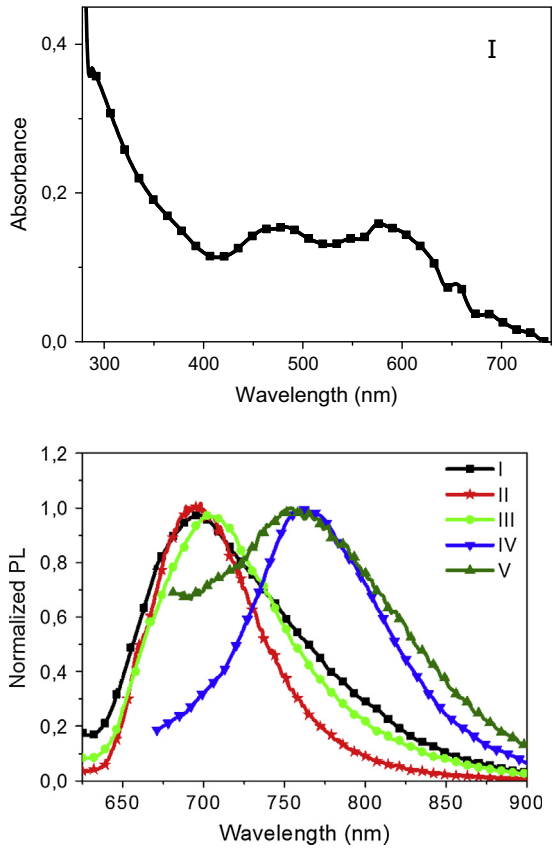

Figure 2 UV–Vis absorption spectrum of 4×10^{-5} M DMF solution of complex **I** and normalized photoluminescence spectra of the complexes in DMF.

Table 5 Absorption and emission data of the Ru(II) complexes in DMF.

Complex	λ_{max}, (nm) ($\varepsilon/10^4$ M^{-1} cm^{-1})		Emiss λ_{max} (nm)	Φ_f
	$\pi \rightarrow \pi^*$	d $\pi \rightarrow \pi^*$		
I	273 (1.72) 290 (0.40)	496 (0.39) 577 (0.40)	697	0.010
II	272 (1.48)	560 (0.59)	696	0.025
III	288 (1.21)	471 (0.39) 578 (0.42)	743	0.009
IV	282 (2.21) 294 (1.32)	350 (0.20) 582 (0.09)	768	0.024
V	293 (2.77)	360 (0.89) 575 (0.29)	754	0.045

deformation vibrations found at (1236–1203) cm^{-1} (ρ_tNH_2), (1154–1031) cm^{-1} (ρ_wNH_2) and (767–759) cm^{-1} (ρ_rNH_2) to higher frequencies (Table 1) (Nakamoto, 1986). In addition, complexes **I** and **II** showed characteristic vibration peaks for the coordinated SCN (νSCN) at 2125 and 2095 cm^{-1}. The bands appeared at 555–619 cm^{-1} may be assigned for M—N bonding, while the band appeared at 652 cm^{-1} in complex **IV** may be assigned for M—O bonding (Ali et al., 2002).

3.2. Mass spectra of complex

The major fragmentations of the complexes are listed in Table 2. The molecular ion peaks of the complexes appeared as in the following: **I**, 522 (M—3H); **II**, 478 (M^+); **III**, 584 (M—H); **IV**, 526 (M—3H); **V**, 632 (M^+). In addition, the mass spectra of the complexes showed the m/e peaks of the ligands: 152 (DABA), 156 (bipy), 137 (anth) 58 (NCS) and the stable Ru isotopes (96, 98, 99, 101, 102, 104).

3.3. Thermal analysis

The thermal studies of the ruthenium complexes are carried out to investigate the stability of the complexes. Calculation of the thermodynamic parameters was performed by using the integral method of Coats–Redfern and approximation method of Horowitz–Metzger (Coats and Redfern, 1964; Horowitz and Metzger, 1963). The temperature ranges of

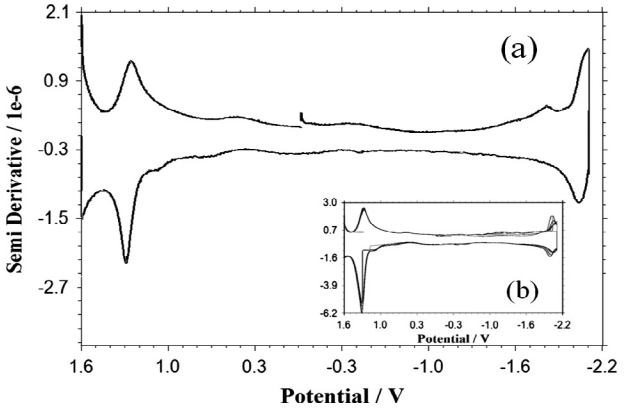

Figure 3 (a) Differential cyclic voltammogram of complex **I** measured in DMF solution, (b) 5 consecutive cyclic voltammograms of complex **I** in DMF solution. The couple at 0.65 V *vs.* Ag/Ag^+ is due to ferrocenium/ferrocene couple, which was used as an internal standard; scan rate is 100 mV s^{-1}.

Table 6 Electrochemical data of the Ru(II) complexes in DMF.

Complex	E_{OX1} (V)	E_{OX2} (V)	E_{OX3} (V)	$E_{RE(1)}$ (V)	$E_{RE(2)}$ (V)	$E_{RE(3)}$ (V)	$E_{RE(4)}$ (V)	HOMO (eV)	LUMO (eV)
I	0.71	1.04	1.27	−1.47	−1.79	−2.09	–	−4.86	−2.68
II	0.70	0.97	1.24	−1.45	−1.80	−1.98	–	−4.85	−2.70
III	0.72	1.19	–	−0.31	−1.39	−1.89	−2.00	−4.87	−2.76
IV	0.76	1.30	–	−1.29	−1.98	–	–	−4.91	−2.86
V	0.79	1.33	–	−0.30	−1.44	−1.71	−1.98	−4.94	−2.71

decompositions along with the corresponding mass loss of species are given in Table 3. A representative TG and DrTG (derivative TG) plot of complex **I** is shown in Fig. 1. Complex **I** is decomposed in two steps. The first decomposition step observed at 347.40–609.48 K is attributed to the loss of bipy and NCS groups with mass losses of 214.22% and 41.31%, respectively. This is followed by the second step with the loss of DABA and NCS groups with mass losses of 210.22% and 40.35%, respectively at 608.48–689.35 K, leaving Ru as the metallic residue (18.34%) (Soliman et al., 2007; Soliman, 2007). Similar trends are observed in the thermal decomposition of complexes II and V, with Ru or RuO_2 as the metallic residues. The temperature ranges of decomposition along with the corresponding mass losses of species are given in Table 3. Thermodynamic parameters of the five complexes are summarized in Table 4. The complexes showed low thermal stability which is reflected from the relatively lower overall activation energy. The entropy change (ΔS^*) for the formation of the activated complexes from the starting reactants is, negative. The negative sign of the ΔS^* suggests that the degree of structural randomness of the activated complex was lower than that of the starting reactants (more disorder, random) and the decomposition reactions are slow reactions (Soliman et al., 2006; Valaev and Gospodinov, 2001).

3.4. UV/visible absorption and fluorescence spectra

The UV–Vis absorption and emission spectra of ruthenium complexes in DMF solvents are shown in Fig. 2. The maximum absorption wavelengths and the molar extinction coefficients are summarized in Table 5. All of the complexes show visible bands in the 350–580 nm regions due to metal-to-ligand charge transfer (MLCT) (Klein et al., 2004; Nazeeruddin et al., 2004). The lowest energy MLCT absorption bands are attributed to the filled metal t_{2g} orbital to the empty π^* orbitals of the 3,4-diaminobenzoic acid and 2-aminobenzoate for the complexes **I**, **II**, **III**, **V** and **IV**, respectively (Fantacci et al., 2003). The lowest-energy MLCT band of ruthenium complex **IV** is slightly red-shifted to 582 nm when compared with other complexes. The redshift is attributed to ligand-field strengths of the σ-donating 2-aminobenzoate ligand (Lesh et al., 2011). The related classes of ruthenium(II) complexes that contain mixtures of bipyridine and phenanthroline typically show the lowest-energy MLCT band between 520 and 540 nm (Klein

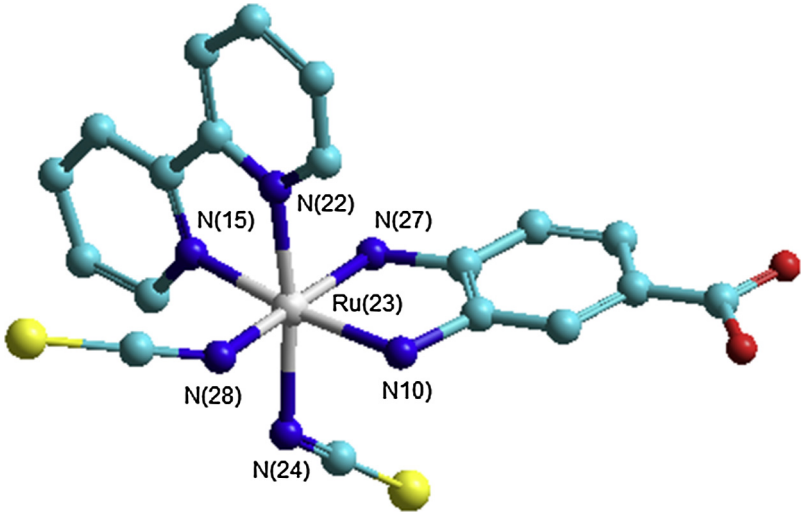

Figure 4 The molecular structure of complex **I** along with the atom numbering scheme.

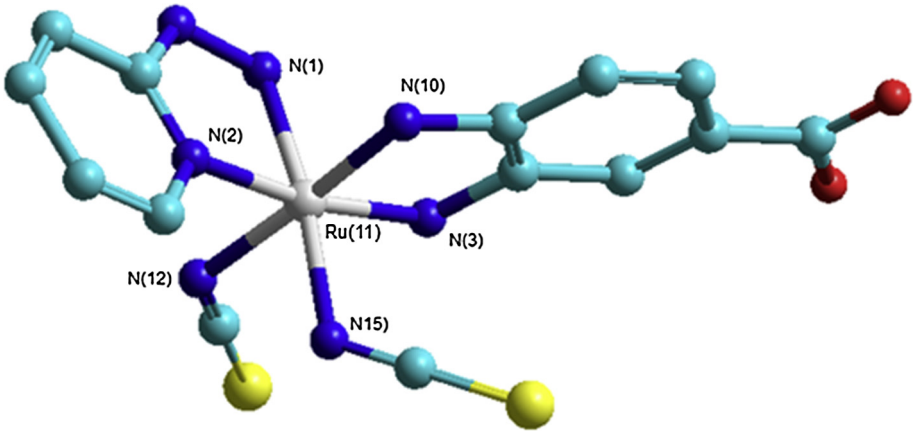

Figure 5 The molecular structure of complex **II** along with the atom numbering scheme.

et al., 2004; Li et al., 2008) whereas synthesized ruthenium(II) complexes with some dinitrogen ligands; 3,4-diamino benzoic acid, 2-hydazinopyridine and anthranilic acid are redshifted due to the ligand-field strengths of ligands. The emission spectra of the ruthenium complexes were obtained at room temperature by excitation at their lowest energy MLCT absorption maxima band. The emission spectra of the complexes containing NCS group *i.e.* complexes **I** and **II** show bands around 697 nm. The emission maxima of complexes containing two carbonyl groups (**III**, **IV** and **V**) are red-shifted compared to other complexes due to stronger acceptor properties of the carbonyl group lowering the energy of the excited state (Nazeeruddin et al., 2004). The emission quantum yield of ruthenium complexes was calculated according to the Eq. (1), where Φ_f is the fluorescence quantum yield, A is the absorption intensity, S is the integrated emission band area and n is the solvent reflective index, u and s refer the unknown and standard, respectively (Karapire et al., 2003).

$$\Phi_f = \Phi_{fs} \frac{S_u}{S_s} \frac{A_s}{A_u} \frac{n_u^2}{n_s^2} \quad (1)$$

The quantum yield measurements for solutions were prepared in DMF and $[Ru(bpy)_3](PF_6)_2$ was used as the reference (Φ = 9.5% in acetonitrile) (Swanick et al., 2012). The calculated values are in the range of 0.9–2.5% and are in agreement with the reported values for ruthenium complexes containing bipyridine ligands (Lee et al., 2003).

3.5. Electrochemical properties

The redox potentials of complexes are summarized in Table 6 and the cyclic voltammogram of complex **I** in DMF is given in Fig. 3. The cyclic voltammogram of complexes **I** and **II** shows three oxidation and three reduction peaks around 0.71, 1.04, 1.27 and −1.47, −1.79, −2.09 *vs.* Ag/Ag^+, respectively. The oxidation peaks are attributed to the amine moiety (N—H) of the ligand, the Ru (II/III) and Ru (III/IV) couples (Lesh et al., 2011; Smith and Masheder, 1976; Sahin et al., 2013; Zourab et al., 2005) whereas the reduction peaks are assigned to the reduction of carboxylic acid protons, carbonyl group and the bipyridine, respectively (Klein et al., 2004; Nazeeruddin et al., 2004). The redox potentials of complexes containing two carbonyl groups, *i.e.* **III**, **IV** and **V** are slightly shifted to anodic area when compared to the others which is attributed to stronger acceptor properties of the carbonyl

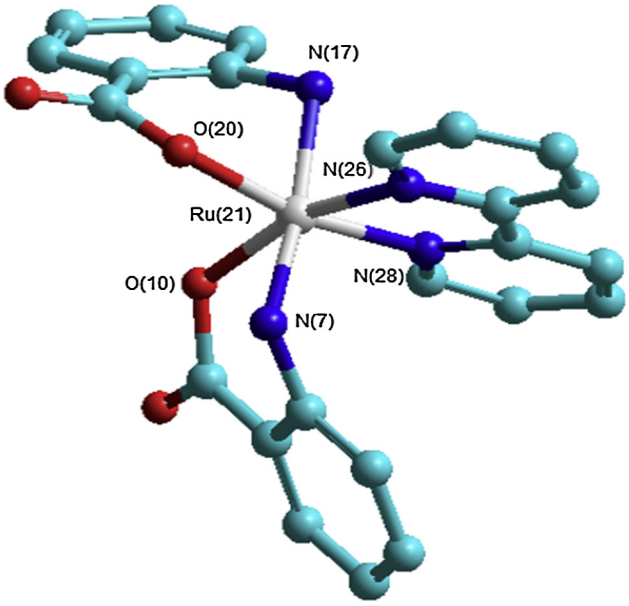

Figure 7 The molecular structure of complex **IV** along with the atom numbering scheme.

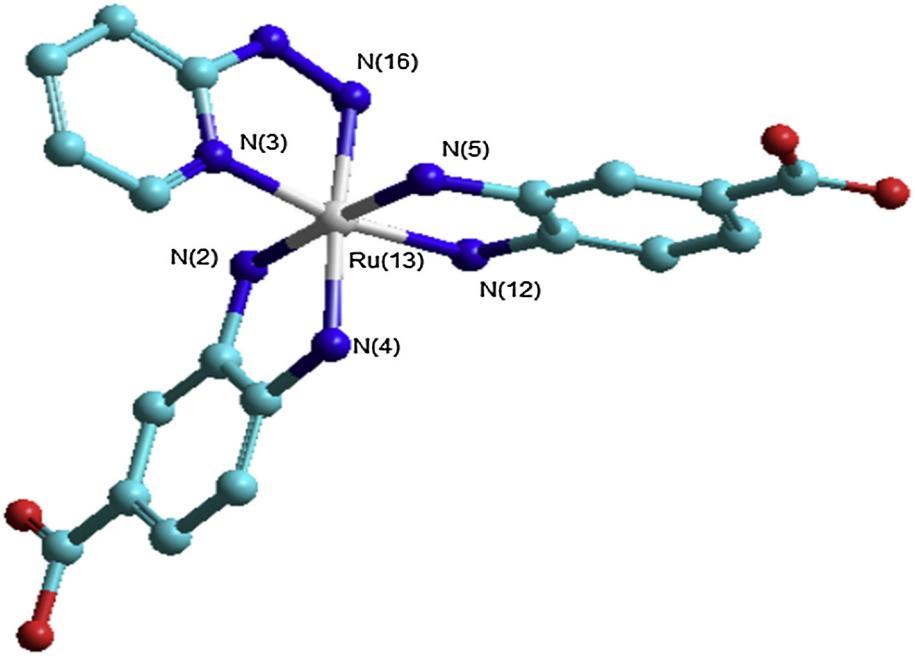

Figure 6 The molecular structure of complex **III** along with the atom numbering scheme.

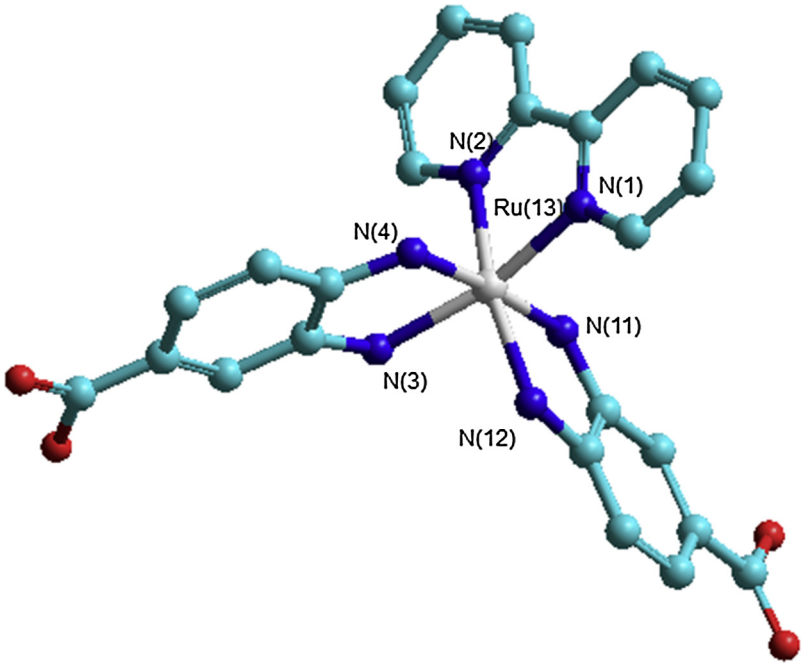

Figure 8 The molecular structure of complex **V** along with the atom numbering scheme.

groups of the complexes (Nazeeruddin et al., 2004). This results in a decrease in the energy of the LUMO energy of the ligand. The cyclic voltammogram of complexes **III** and **V** shows an additional reduction peak at −0.30 eV, which is attributed to the chloride ion in the second coordination sphere of ruthenium complex. The chloride ion interacts with Ag electrode surface and leads to the reduction of the chloride (Arai et al., 1996). The HOMO and LUMO energy levels of the complexes were calculated using the maximum of first oxidation and reduction potentials (Sahin et al., 2013). Ferrocene was used as an internal standard (0.65 V *vs.* Ag/Ag^{+}). The calculated HOMO and LUMO energy levels of the complexes are in the range of −4.94 to −4.85 eV and −2.86 to −2.68 eV, respectively. Consecutive cyclic behavior of the complexes was also investigated in order to determine their electrochemical stability. No significant change in peak currents and potentials of anodic and cathodic areas are observed (Fig. 3b). Although the energy states and electrochemical stability of the complexes are appropriate to be used as photosensitizers in DSSCs, the limited solubility of them hinders their utilization in this application area. Nevertheless, the HOMO and LUMO energy levels and thermal stabilities of all of the complexes show that they may find application in vacuum evaporated organic photonic systems. The low lying HOMO energy levels will allow hole injection from commonly used hole transport layers, *e.g.* PEDOT:PSS whereas the LUMO energy levels are appropriate to gain electron from metals with high work function and widely used electron transport materials, *e.g.* Ca, TPBi, BPhen, *etc.* (Oner et al., 2011, 2012; Saygili et al., 2011, 2012).

3.6. Molecular modeling

In the absence of a crystal structure and to obtain the molecular conformation of the complexes, energy minimization studies were carried out on the basis of the semi-empirical PM3 level provided by HyperChem 7.5 software. The molecular structure of complexes along with the atom numbering scheme is given in Figs. 4–8.

4. Conclusion

Here, we reported the synthesis, thermodynamic, spectroscopic and electrochemical properties of new ruthenium(II) complexes with some dinitrogen ligands. The complexes have been proven to have an octahedral geometry in which the six coordination sites are occupied by the ligands where DABA, bipy and anthranilic acid as bidentate ligands, and the coordinated thiocyanate as monodentate ligand. The absorption spectrum of ruthenium complex **IV** shows redshift compared with other complexes due to more ligand-field strengths of the σ-donating 2-aminobenzoate ligand. The calculated energies of the HOMO and LUMO are in the range of −4.94 to −4.85 eV and −2.86 to −2.68 eV. The obtained results show that there is an important effect of different dinitrogen ligands on molecular modeling, spectroscopic and electrochemical properties of the complexes.

References

Ali, M.A., Livingstone, S.E., 1974. Metal complexes of sulphur–nitrogen chelating agents. Coord. Chem. Rev. 13, 101–132.

Ali, S.A., Soliman, A.A., Ali, M.A., Ramadan, M.R., 2002. Chromium, molybdenum and ruthenium complexes of certain Schiff bases. J. Coord. Chem. 55, 1161–1170.

Arai, K., Kusu, F., Noguchi, N., Takamura, K., Osawa, H., 1996. Selective determination of chloride and bromide ions in serum by cyclic voltammetry. Anal. Biochem. 240, 109–113.

Balzani, V., Juris, A., Venturi, M., Campagna, S., Serroni, S., 1996. Luminescent and redox-active polynuclear transition metal complexes. Chem. Rev. 96, 759–834.

Campbell, M.J.M., 1975. Transition metal complexes of thiosemicarbazide and thiosemicarbazones. Coord. Chem. Rev. 15, 279–319.
Chao, H., LN, Ji., 2005. DNA interactions with ruthenium(II) polypyridine complexes containing asymmetric ligands. Bioinorg. Chem. Appl. 3, 15–28.
Coats, A.W., Redfern, J.P., 1964. Kinetic parameters from thermogravimetric data. Nature 201, 68–69.
Crichton, R., 2012. In: Biological inorganic chemistry, second ed. Elsevier, Belgium, pp. 69–89.
De Cola, L., Belser, P., 1998. Photoinduced energy and electron transfer processes in rigidly bridged dinuclear Ru/Os complexes. Coord. Chem. Rev. 177, 301–346.
Dos Santos, E.R., Mondelli, M.A., Pozzi, L.V., Corrêa, R.S., de-Araújo, H.S.S., Pavan, F., Leite, C.Q.F., Ellena, J., Malta, V.R.S., Machado, S.P., Batista, A.A., 2013. New ruthenium(II)/phosphines/diimines complexes: promising antitumor (human breast cancer) and *Mycobacterium tuberculosis* fighting agents. Polyhedron 51, 292–297.
Fantacci, S., Angelis, F.D., Selloni, A., 2003. Absorption spectrum and solvatochromism of the [Ru(4,4′-COOH-2,2′-bpy)$_2$(NCS)$_2$] molecular dye by time dependent density functional theory. J. Am. Chem. Soc. 125, 4381–4387.
Gratzel, M., 2004. Solar energy conversion by dye-sensitized photovoltaic cells. Inorg. Chem. 44, 6841–6851.
Horowitz, H.H., Metzger, G., 1963. A new analysis of thermogravimetric traces. Anal. Chem. 35, 1464–1468.
HyperChem version 7.5 Hypercube, Inc. 2003.
Juris, A., Balzani, V., Barigelletti, F., Campagna, S., Belser, P., Zelewsky, A.V., 1988. Ru(II) polypyridine complexes: photophysics, photochemistry, eletrochemistry, and chemiluminescence. Coord. Chem. Rev. 84, 85–277.
Kaes, C., Katz, A., Hosseini, M.W., 2000. Bipyridine: the most widely used ligand. A review of molecules comprising at least two 2,2′-bipyridine units. Chem. Rev. 100, 3553–3590.
Kalyanasundaram, K., Grätzel, M., 1998. Applications of functionalized transition metal complexes in photonic and optoelectronic devices. Coord. Chem. Rev. 177, 347–414.
Karapire, C., Timur, C., Icli, S., 2003. A comparative study of the photophysical properties perylenediimides in liquid phase, PVC and sol–gel host matrices. Dyes Pigm. 56, 135–143.
Klein, C., Nazeeruddin, M.K., Di Censo, D., Liska, P., Grätzel, M., 2004. Amphiphilic ruthenium sensitizers and their applications in dye-sensitized solar cells. Inorg. Chem. 43, 4216–4226.
Lee, K.W., Slinker, J.D., Gorodetsky, A.A., Flores-Torres, S., Abruna, H.D., Houstona, P.L., Malliaras, G.G., 2003. Photophysical properties of tris(bipyridyl)ruthenium(II) thin films and devices. Phys. Chem. Chem. Phys. 5, 2706–2709.
Lesh, F.D., Allard, M.M., Shanmugam, R., Hryhorczuk, L.M., Endicott, J.F., Schlegel, H.B., Verani, C.N., 2011. Investigation of the electronic, photosubstitution, redox, and surface properties of new ruthenium(II)-containing amphiphiles. Inorg. Chem. 50, 969–977.
Li, X., Gui, J., Yang, H., Wud, W., Li, F., Tian, H., Huang, C., 2008. A new carbazole-based phenanthrenyl ruthenium complex as sensitizer for a dye-sensitized solar cell. Inorg. Chim. Acta 361, 2835–2840.
McCleverty, J.A., Meyer, T.J., 2004. In: Comprehensive Coordination Chemistry. II: From Biology to Nanotechnology, vol. 5. Elsevier Ltd, Oxford, p. 556.
Metcalfe, C., Thomas, J.A., 2003. Kinetically inert transition metal complexes that reversibly bind to DNA. Chem. Soc. Rev. 32, 215–224.
Nakamoto, K., 1986. Infrared and Raman Spectra of Inorganic and Coordination Compounds, fourth ed. Wiley, New York, p. 206.
Nazeeruddin, M.K., Key, A., Rodicio, I., Humphry-Baker, R., Müller, E., Liska, P., Vlachopoulos, N., Grätzel, M., 1993. Conversion of light to electricity by cis-X$_2$bis(2,2′-bipyridyl-4,4′-dicarboxylate)ruthenium(II) charge-transfer sensitizers (X = Cl-, Br-, I-, CN-, and SCN-) on nanocrystalline titanium dioxide electrodes. J. Am. Chem. Soc. 115, 6382–6390.
Nazeeruddin, M.K., Zakeeruddin, S.M., Lagref, J.J., Liska, P., Comte, P., Barolo, C., Viscardi, G., Schenk, K., Grätzel, M., 2004. Stepwise assembly of amphiphilic ruthenium sensitizers and their applications in dye-sensitized solar cell. Coord. Chem. Rev. 248, 1317–1328.
Oner, I., Varlikli, C., Icli, S., 2011. The use of a perylenediimide derivative in both hole and electron transport layers of ITO/PEDOT:PSS/PVK/Alq$_3$/LiF/Al electroluminescent device. Appl. Surf. Sci. 257, 6089–6094.
Oner, I., Sahin, C., Varlikli, C., 2012. Electroluminescence from two new ruthenium(II) complexes as phosphorescent dopant: positive effect of swallow-tail bipyridyl ligand. Dyes Pigm 95, 23–32.
O'Regan, B., Grätzel, M., 1991. A low-cost, high-efficiency solar cell based on dye-sensitized colloidal TiO$_2$ films. Nature 353, 737–740.
Padhye, S., Kauffman, G.B., 1985. Transition metal complexes of semicarbazones and thiosemicarbazones. Coord. Chem. Rev. 63, 127–160.
Robertson, N., McGowan, C.A., 2003. A comparison of potential molecular wires as components for molecular electronics. Chem. Soc. Rev. 32, 96–103.
Sahin, C., Ulusoy, M., Zafer, C., Ozsoy, C., Varlikli, C., Dittrich, T., Cetinkaya, B., Icli, S., 2010a. The synthesis and characterization of 2-(2′-pyridyl)benzimidazole heteroleptic ruthenium complex: efficient sensitizer for molecular photovoltaics. Dyes Pigm. 84, 88–94.
Sahin, C., Dittrich, T., Varlikli, C., Icli, S., Lux-Steiner, M.C., 2010b. Role of side groups in pyridine and bipyridine ruthenium dye complexes for modulated surface photovoltage in nanoporous TiO$_2$. Sol. Energy Mater. Sol. Cells 94, 686–690.
Sahin, C., Varlikli, C., Zafer, C., Shi, Q., Douthwaite, R.E., 2013. A new 1H-pyridin-(2E)-ylidene ruthenium complex as sensitizer for a dye-sensitized solar cell. J. Coord. Chem. 66, 1384–1395.
Saygili, G., Ozsoy, C., Oner, I., Zafer, C., Varlikli, C., Icli, S., 2011. Enhanced electroluminescence from MEH-PPV-POSS:CuInS$_2$ nanocomposite based organic light emitting diode. Synth. Met. 161, 196–202.
Saygili, G., Varlikli, C., Zafer, C., Ozsoy, C., 2012. Highly efficient MEH-PPV-POSS based PLEDs through optimization of charge transport. Synth. Met. 162, 621–629.
Smith, J.R.L., Masheder, D., 1976. Amine oxidation. Part IX. The electrochemical oxidation of some tertiary amines: the effect of structure on reactivity. J. Chem. Soc. Perkin Trans. 2, 47–51.
Soliman, A.A., 2007. Spectral and thermal studies on ruthenium carbonyl complexes with 5-trifluoromethyl-2,4-dihydropyrazol-3-one ligands. Spectrochim. Acta 67A, 852–857.
Soliman, A.A., Samir, M.E., Ali Omyma, A.M., 2006. Thermal study of chromium and molybdenum complexes with some nitrogen and nitrogen-oxygendonors ligands. J. Therm. Anal. Calorim. 83 (2), 385–392.
Soliman, A.A., Khattab, M.M., Ramadan, R.M., 2007. Complexes of ruthenium and molybdenum carbonyls with some pyridylamine derivatives. Transit. Met. Chem. 32, 325–331.
Swanick, K.N., Ladouceur, S., Zysman-Colman, E., Ding, Z., 2012. Bright electrochemiluminescence of iridium(III) complexes. Chem. Commun. 48, 3179–3181.
Valaev, L.T., Gospodinov, G.G., 2001. Study on the kinetics of the isothermal decomposition of selenites from IIIB group of the periodic system. Thermochim. Acta 370 (1), 15–19.
Vos, J.G., Kelly, J.M., 2006. Ruthenium polypyridyl chemistry; from basic research to applications and back again. Dalton Trans., 4869–4883
Zourab, S.M., Ezzo, E.M., El-Aila, H.J., Salem, J.K.J., 2005. Study of the kinetics of oxidation of amines by potassium ferricyanide in the presence of N, N-dimethyldodecylamine N-oxide. J. Surf. Detergt. 8, 83–89.